EPJ Web of Conferences **287**, 08017 (2023) https://doi.org/10.1051/epjconf/202328708017
EOSAM 2023

Featurization of Ultrafast Expansion and Geometrical Properties of Heterogeneous Colliding Plasmas

Haider M. Al-Juboori[1,*] , *Tom McCormack* [2]

[1] Department of Electronics Engineering and Communications, South East Technological University, Carlow, Ireland.
[2] School of Physics, University College Dublin, Belfield, Dublin, Ireland.

Abstract. Numerous fields of research and industry have undergone revolutionary change because of the unique characteristics of ultrashort laser pulses. Moreover, the ultrafast imaging sensors, such as ICCD technique, can help to understand the ionization features and expansion properties of colliding laser-induced plasma (CLPP) and related stagnation layer (S.L.) geometry. In this work, the effort will be focused on CLPP experiments from two seeds of heterogeneous elements. The research's goal is to analyse the geometrical development of the colliding plasma, the temporal evolution of plume composition features and its associated characteristics. The expansion velocity and forward propagation range (FPR) of the stagnation layer in a nanosecond scale—both of which have been discovered. The ultrafast imaging results give the sight and explain the possibilities of extant technologies that can help to re-engineer the plasma characteristics for the next generation of lithography applications or new selective physical concepts.

1 Introduction

The effect of the atomic mass of the ablating target on the formation and expansion of the interaction region in laterally colliding plasmas has been focused on many scientific contributions, where several techniques and setups were applied to achieve colliding laser-produced plasmas of different elements [1-4]. Some reasons behind these studies focused on the possibility to enhance specific emission lines from one of the dual materials by introducing the presence of the other target material or used the outcomes for particular applications of nano-composites, additionally, investigated the plume-front velocity in different environments as well as the effect of the different surrounding media on the electron density and its temperature. The present work will be focused on colliding plasmas create from two seeds of heterogeneous flat targets where Nd:YAG Laser with a pulse duration of ~5 ns and λ= 1064 nm was used.

2 Methodology

A detailed description of the digital nanosecond imaging architecture of colliding laser-produced plasma can be found it in Refs. [5,3]. Figure 1 explains the temporal evolution example of the Si-Al stagnation layer and its related features using a bandpass filter 450 nm.
Figure 2 shows the visible intensity emission using six different bandpass filters bandwidths. It is also evident in this figure that the majority of the species emission is in the bandwidth of the 450nm and 400nm filters. This contains more than 60% of total emission at different laser energies.

3 Results

All the digital analysis was performed using advanced codes inside the MATLAB digital environment.

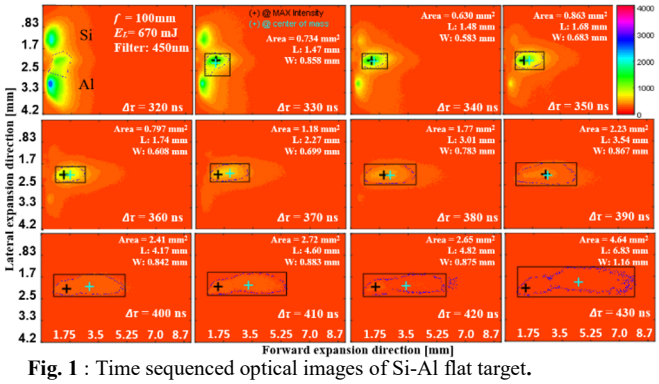

Fig. 1 : Time sequenced optical images of Si-Al flat target.

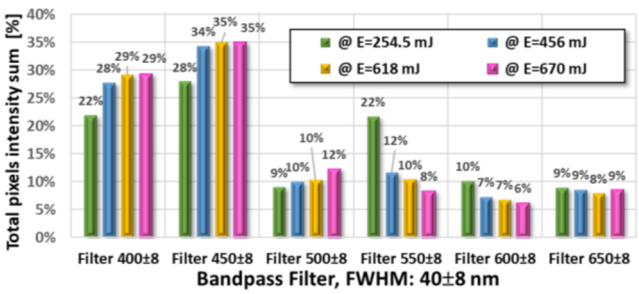

Fig. 2 : Percentage of the total intensity sum of multi-elements Si-Al stagnation layer, (Δτ = 330ns to 430ns), D = 1.66 mm.

The spatial evolution of the S.L. centroid at four different laser energies illustrated in Figure 3. Each data point is the centroid position at 10 ns intervals starting from 320 ns and ending at 430 ns. In the same figure one can observe the largest propagation distance in forward expansion direction (FED) in case of the lowest value of laser energy pulse (*i.e.*, E_L= 254 mJ). A Special digital algorithm was built to track the expansion velocity of the Si-Al stagnation region. The expansion velocity experiments were done using the 450nm filter. Figure 4a and Figure 4c show the creation moment of the hybrid stagnation layer at Δτ = 320 ns for two different seed separation (D).

* Corresponding author: haider.aljuboori@setu.ie

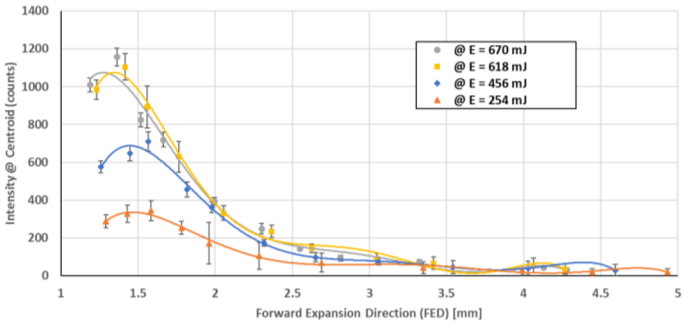

Fig. 3 : The peak visible emission at stagnation layer centroid as a function of distance using filter 450nm at D = 1.66 mm.

It is clear, the interaction zone starts formation earlier at the seed separation of 1.66mm. The stagnation layer density seems more intense and has a bigger area at D=2.16 mm and Δτ=350ns if compared with the same case at D=1.66mm, as shown in Figure 4b and Figure 4d.

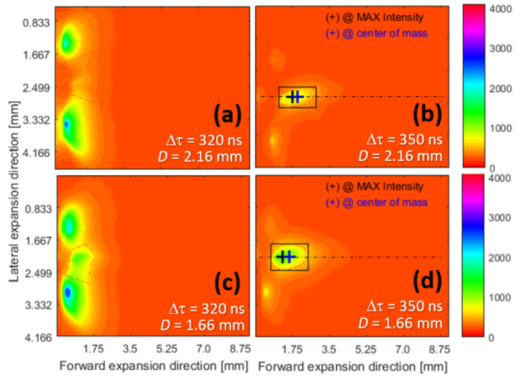

Figure 4: Visible images of Si-Al colliding plasma using 450nm at E_L = 670 mJ at two difference seed separation D = 2.16mm and 1.66mm.

Figure 5 shows the group behaviour and displacement range of the multifarious ionic species inside the Si-Al stagnation layer (red●▲), obtained using the 450nm filter, and the centroid velocity (blue▲) is observed to be smaller than the max/e velocity (blue●).

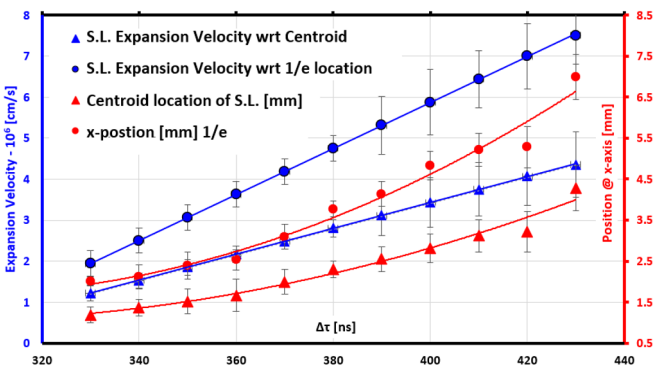

Figure 5: Si-Al stagnation layer expansion features through the temporal evolution at laser energy = 670 mJ.

The velocity of expansion tends to decrease with increasing laser energy as explained in Figure 6. From the linear fit shown in Figure 6, the dropping rate of the $v_{avg.exp}$ per unit laser energy is around ~$3.51{\cdot}10^3$ cm/s for each one millijoule (mJ) at max/e and will be ~2.45·103 (cm/s) per millijoule (mJ) at centroid at D =1.66 mm.

Table 1 compares the stagnation layer dynamic at quasi-similar laser power density at two different seed separation values (i.e. using D = 1.66 mm, and D=2.16mm), where the average expansion velocity has a higher value by 40% at shorter separation distance (i.e. D = 1.66 mm) if compared with $v_{avg.exp}$ value at D=2.16mm where $v_{avg.exp}$ = $4.05{\pm}0.34{\cdot}10^6$ cm/s and $2.36{\pm}0.31{\cdot}10^6$ cm/s at max/e and centroid, respectively. In the same scenario, the FPR recorded greater values at E_L=456 mJ and D=1.66 mm for both cases if compared with the values at E_L = 670 mJ and D = 2.16 mm.

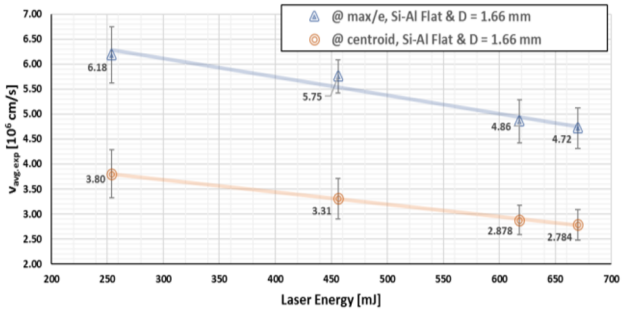

Figure 6: Average expansion velocity of the Si-Al flat stagnation layer in time for different laser energy @ D = 1.66 mm.

Table 1: Forward propagation range and $v_{avg.exp}$ for Si-Al target.

Laser Energy (mJ)	Laser Power Density (TW/cm²)	D (mm)	FPR @max/e (mm)	FPR @centro (mm)	$v_{avg.exp}$ @max/e (mm)	$v_{avg.exp}$ @centro (mm)
456	3.05	1.66	5.499	3.359	$5.8{\pm}0.3{\cdot}10^6$	$3.3{\pm}0.4{\cdot}10^6$
670	2.94	2.16	4.183	2.408	$4.1{\pm}0.3{\cdot}10^6$	$2.4{\pm}0.3{\cdot}10^6$

4. Concluding Remarks

The present study based on ultrafast optical imaging techniques provides a considerable amount of detailed data related to the geometrical analysis and expansion velocity of the interaction zone. According to the above work, a brief explanation on the formation and evolution mechanism of the Si-Al plasma was illustrated based on two different seed separations (i.e. D =1.66 and D =2.16) using bandpass filter 450nm for different laser energies.

The expansion velocities difference between the plasma at centroid and max/e front is caused by a pressure gradient in the plasma inside the interaction zone, where the plasma core, based on centroid location, is in a high-pressure region and the plasma front is freely expanding into a vacuum. It is also evident that the expansion of the Si-Al plasma at the centroid position and max/e front does not satisfy a linear relationship using 450nm filter for different laser power densities.

References

[1] P. K. Pandey, R. K. Thareja, and J. T. Costello, "Heterogeneous (Cu-Ti) colliding plasma dynamics," Physics of Plasmas, vol. 23, no. 10, p. 103516, 2016.

[2] A. Mondal *et al*, "Spectroscopic investigation of stagnation region in laterally colliding plasmas" Physics of Plasmas, vol. 26, no. 2, p. 022102, 2019.

[3] Al-Juboori, H., and T. McCormack. "Expansion Dynamic of Stagnation Layer in Colliding Plasmas: Dependence of Observation Bandwidth and Plasma Plume Separation." In Jour. of Physics: vol. 2407, no. 1, p. 012003. IOP Publishing, 2022.

[4] P. K. Pandey, R. K. Thareja, R. P. Singh and J. T. Costello, "Deposition of nanocomposite Cu–TiO 2 using heterogeneous colliding plasmas," Applied Physics B, vol. 124, no. 3, p. 50, 2018.

[5] Al-Juboori, H., and T. McCormack. "Digital nanosecond imaging architecture and analytical tracking technique of colliding laser-produced plasma." Optical and Quan. Elec. 54, no. 5 (2022): 321.